# Syntheses, Crystal Structures and Characterization of Two Coordination Polymers Based on Mixed Ligands

WANG Yu-Fang[1] (王玉芳);HE Chao-Jun[2] (何朝军)

[1] *College of Chemistry and Chemical Engineering, and Henan Key Laboratory of Function-oriented Porous Materials, Luoyang Normal University, Luoyang* 471934, *China;*[2] *School of Food and Drug, Luoyang Normal University, Luoyang, Henan* 471934, *China*

**ABSTRACT** Two new coordination polymers, namely, $\{[Cd_{1.5}(bc)_2(HL)].H_2O\}_{2n}$ (**1**) and $[Mn(ip)(H_2L)(H_2O)]_n$ (**2**) ($H_2L$ = 3-(1H-pyrazol-4-yl)-5-(pyridin-2-yl)-1,2,4-triazole, Hbc = benzoic acid, $H_2ip$ = isophthalic acid) were constructed by solvothermal reaction. The compounds were characterized by elemental analysis, FT-IR spectroscopy, and single-crystal X-ray diffraction. Compound **1** displays a two-dimensional plane structure consisting of $[Cd_3(bc)_2(HL)]$ subunits. Compound **2** possesses a one-dimensional chain structure and is further extended into a 3-D supramolecular architecture via hydrogen bonds. Moreover, photoluminescence studies showed compound **1** exhibits luminescent emissions with emission maxima at 375 nm. Magnetic susceptibility measurements of **2** indicate that domain antiferromagnetic interactions exist between Mn(II) ions. In addition, thermogravimetric properties of **1** and **2** were also measured.

**Keywords: cadmium(II); manganese(II); crystal structure; luminescence; magnetic property**

**DOI:10.14102/j.cnki.0254-5861.2011-1773**



## 1 INTRODUCTION

The design and synthesis of new coordination polymers are nowadays a challenging research topic that attracts increasing interest due to the creation of various intriguing architectures and their potential applications[1-7] of such metal-organic materials. As we all know, the selection of organic ligands is very important in the construction of coordination polymers. Recently, N-donor ligands have been widely employed

Received 5 July 2017; accepted 16 October 2017 (**CCDC 1535311 for 1 and 1560119 for 2**)

① This work was financially supported by the National Natural Science Foundation of China (21571093), and the Science and Technology Project of Henan Province (No. 162106000025)

② Corresponding author. Wang Yu-Fang. E-Mail: wangyf78@163.com

in the construction of coordination polymers or metal-organic frameworks with intriguing structure. To modulate the structure, different polycarboxylate ligands can be used as auxiliary ligands to direct the self-assembly. Although these appealing topology and interesting properties of metal coordination frameworks that have been synthesized by various N-donor ligands and aromatic carboxylic acid have so far been explored to a great extent in the area of crystal engineering to date[8-11], the synthesis of compositionally and structurally designed MOFs and their composites remains a significant challenge nowadays owing to the difficulty in fine-tunning the phase distributions and architectures of the final products. We selected 3-(1H-pyrazol-4-yl)-5-(pyridin-2-yl)-1,2,4-triazole as ligand and benzoic and isophthalic acids as auxiliary ligands in this paper. Herein we synthesized two new coordination polymers, $\{[Cd_{1.5}(bc)_2(HL)]\cdot H_2O\}_{2n}$ (**1**) and $[Mn(ip)(H_2L)(H_2O)]_n$ (**2**). Those structure inducing physical properties, like thermal stability, photoluminescence, magnetic properties and so forth is also described and discussed.



## 2 EXPERIMENTAL

### 2. 1 Materials and characterization

All reagents were of analytical grade and used without further purification. Elemental analyses for carbon, hydrogen and nitrogen atoms were carried out on a Vario EL Ⅲ elemental analyzer. The IR spectrum was recorded (400～4000 $cm^{-1}$ region) on a SHIMADZU IR Affinity-1S Spectrometer. All fluorescence measurements were carried out on an F-7000 Fluorescence Spectrophometer (220 ～ 240V). Thermogravimetric analyses (TGA) were carried out in nitrogen at a heating rate of 10 °C·$min^{-1}$ using a TG/DTA 6300 integration thermal analyzer. Variable-temperature magnetic susceptibilities were measured on a MPMS-7 SQUID magnetometer. Diamagnetic corrections were made with Pascal's constants for all constituent atoms.

### 2. 2 Preparation of $\{[Cd_{1.5}(bc)_2(HL)]\cdot H_2O\}_{2n}$ (1)

A mixture of $Cd(NO_3)_2\cdot 4H_2O$ (92.5 mg, 0.30 mmol), $H_2L$ (21.2 mg, 0.10 mmol), Hbc (36.6 mg, 0.30 mmol) and KOH (11.2 mg, 0.2 mmol) was dissolved in $H_2O$, added in a 10 mL small glass bottle after stirring and then sealed in a 25 mL Teflon-lined stainless-steel autoclave at 130 ℃ for 72 h, followed by slowly cooling to room temperature at a rate of 5 °C·$h^{-1}$. Light yellow block-shaped crystals were obtained in 54% yield, washed with water and air-dried. IR ($cm^{-1}$): 3433(w), 3180(w), 2976(w), 2363(m), 2336(m), 1581(m), 1536(m), 1526(m), 1383(m), 1300(m), 1150(m), 1069(m), 1025(m), 952(m), 848(m), 765(m), 710(m), 670(m),

518(m), 473(m). Anal. Calcd. (%) for $C_{24}H_{19}Cd_{1.5}N_6O_5$: C, 45.03; H, 2.99; N, 13.13. Found (%): C, 45.55; H, 2.92; N, 13.10.

### 2. 3 Preparation of $[Mn(ip)(H_2L)(H_2O)]_n$ (2)

The preparation of **2** was similar to that of **1** except that $MnSO_4 \cdot 4H_2O$ and Hbc were used instead of $Cd(NO_3)_2 \cdot 4H_2O$ and $H_2ip$. Light-brown crystals of **2** were obtained in 50% yield. IR ($cm^{-1}$): 3429 (w), 3056 (w), 2465(m), 2320(m), 1617 (m), 1595 (m), 1558 (m), 1476 (m), 1401 (m), 1308 (m), 1196 (m), 1057 (m),784 (m), 716 (m). Anal. Calcd. (%) for $C_{18}H_{14}MnN_6O_5$: C, 48.12; H, 3.14; N, 18.71. Found (%): C, 48.45; H, 3.12; N, 18.58.

### 2. 4 Crystal structure determination

Single-crystal X-ray diffraction data of compounds **1** and **2** were collected with a Rigaku Oxford SuperNova diffractometer with a Mo$K\alpha$ radiation ($\lambda$ = 0.71073 Å). Intensities were collected and reduced on the program CrysAlisPro (Rigaku Oxford, Version 1.171.39.3a), and a multi-scan absorption correction was applied. The structures were solved by direct methods with SHELXS-97[12] and refined on $F^2$ by full-matrix least-squares with SHELXL-97[13]. All non-hydrogen atoms were refined anisotropically, and all hydrogen atoms were assigned with common isotropic displacement factors and included in the final refinement by use of geometrical restrains. The details of crystal parameters are summarized in Table 1, and the selected bond lengths are listed in Table 2.

## 3 RESULTS AND DISCUSSION

### 3. 1 Structure description

#### 3. 1. 1 Crystal structure of $\{[Cd_{1.5}(bc)_2(HL)] \cdot H_2O\}_{2n}$ (1)

Compound **1** crystallizes in the monoclinic space group $P2_1/n$ and exhibits a 2D layered framework, and its asymmetric unit contains one and a half Cd atoms, one $HL^-$ ligand, two $bc^-$ ligands and one uncoordinated water molecule. As shown in Fig. 1, the two Cd(II) ions in **1** are both six-coordinated, in which the Cd(1) ion with 1/2 occupation is coordinated by two nitrogen atoms (N(4), N(4)#1) of two different $H_2L$ ligands and four oxygen atoms (O(2), O(2)#1, O(3), O(3)#1) from four different Hbc ligands. The Cd(1) is located in an inversion center. While Cd(2) is coordinated by three nitrogen atoms (N(1), N(3), N(6)#2) of two different $H_2L$ ligands and three oxygen atoms (O(1), O(3) and O(4)) from two different $bc^-$ ligands. Besides, the two adjacent Cd(II) atoms are bridged by O(1) and O(2) atoms of carboxylate group from one $bc^-$ ligand and a

bifurcated O(3) atom of carboxylate group from another $bc^-$ ligand, and another O(4) atom of carboxylate group from this $bc^-$ ligand is linked to Cd(2) atom. At the same time, the two adjacent Cd(II) ions are bridged by N(3) and N(4) atoms of triazole from $HL^-$ ligand, and N(1) atom of pyridine from this $HL^-$ ligand is linked to Cd(2) ion. The Cd–O distances fall in the range of 2.1892(19)～2.5890(19) Å, and the Cd–N distances vary from 2.261(2) to 2.403(2) Å. These bond angles and bond distances all fall in the normal ranges[14]. In compound **1**, two pairs of oppositely arranged $bc^-$ anions and one pair of oppositely arranged $HL^-$ anions bind three Cd(II) ions (two Cd(2) and one Cd(1)) to form the $[Cd_3(bc)_2(HL)]$ subunit, with the Cd(1)···Cd(2) separation to be 3.806 Å. Then the trinuclear subunits are linked to form an infinite two-dimensional network by an $HL^-$ ligand bridging mode (Fig. 2).

In addition, in the crystal packing, there are hydrogen bonding interactions among uncoordinated water molecules and nitrogen atoms of $HL^-$ ligands and oxygen atoms of $bc^-$ ligands (N(5)–H(5)···O(5)#1 (H···O/N···O distance = 1.96/2.749(3) Å, angle = 152.3 °); O(5)–H(5A)···N(2)#2 (H···N/O···N distance = 1.94/2.789(3) Å, angle = 171.9 °); O(5)–H(5B)···O(4) (H···O/O···O distance = 1.94/2.738(3) Å, angle = 157.2)). The 2D architecture of **1** is also reinforced by extensive hydrogen bonding interactions.

### 3. 1. 2 Crystal structure of $[Mn(ip)(H_2L)(H_2O)]_n$ (2)

X-ray single-crystal diffraction analysis reveals that **2** crystallizes in monoclinic system, space group $P2_1/n$ and exhibits a 1D framework. As shown in Fig. 3, the asymmetric unit contains one Mn(II) ion, one $H_2L$ ligand and one $ip^{2-}$ ligand. The Mn(II) center is five-coordinated to two nitrogen atoms (N(2) and N(3)) from the same $H_2L$ ligand, three oxygen atoms (O(1), $O(4)^{\#1}$) from two different $H_2ip$ ligands and one oxygen atom (O(5)) from one coordinated water molecule. The Mn–N distances are 2.223(2) and 2.260(2) Å, respectively. And the Mn–O lengths fall in the range of 2.1653(18)～2.2175(18) Å, which fall in the normal range of those observed in manganese complexes[15]. And there are weak coordinated bonds (Mn(1)···O(2) = 2.665 and Mn(1)···O(3) = 2.559 Å) in **2**, resulting in two carboxylate groups of $ip^{2-}$ ligand nearly coplanar. The $H_2L$ ligand adopts the chelating mode to connect one Mn(II) atom through one imidazole N atom and one pyridine N atom. At the same time, two carboxyl groups of $ip^{2-}$ ligand in compound **2** are completely deprotonated and exhibit coordination mode $\mu_2$-$\eta^1$:$\eta^1$ to link two Mn(II) ions, finally forming a one-dimensional chain with the Mn···Mn distances of 10.160 Å.

In the crystal packing, there are H-bonding interactions among pyridine N atom, imidazole N atom, coordinated water molecule and carboxyl groups of $ip^{2-}$ ligand: (N(5)–H(5)···O(2) (H···O/N···O distance = 1.995/2.831 Å, angle = 163.6 °); O(5)–H(5A)···O(1) (H···N/O···O distance = 1.865/2.747 Å, angle = 153.8 °);

O(5)–H(5B)···O(4) (H···N/O···O distance = 1.933/2.756 Å, angle = 162.5); N(7)–H(7)···O(3) (H···N/N···O distance = 2.268/2.918 Å, angle = 132.5°). In addition, $\pi\cdots\pi$ piling interactions exist between the nearest neighboring benzene rings which parallel each other with the interplane distances of 4.070 Å. These hydrogen bonds and $\pi\cdots\pi$ stacking interactions lead to the formation of a 3-D supramolecular network (Fig. 4), in which the Mn···Mn separation is 4.800 Å.

### 3. 2 Luminescence spectra of compound 1

As shown in Fig. 5, the complexes with $d^{10}$ metal centers have been investigated for fluorescent properties and for potential applications as fluorescence emitting materials. It should be noted that $H_2L$ ligand displays fluorescence in the solid state at room temperature, while compound **1** exhibits different fluorescence. The ligand maximum appears at an excitation wavelength $\lambda_{ex}$ = 325 nm, with a maximum emission peak at $\lambda_{em}$ = 380 nm. In **1**, there is an excitation maximum at 270 nm with a maximum emission peak at 375 nm. It can be seen clearly that compared with the ligand $H_2L$, the emission peak of compound **1** has slight blue shift by 380 to 375 nm. The phenomena should be best ascribed to the metal-to-ligand charge transfer according to literatures[16-18].

### 3. 3 Magnetic properties of compound 2

For **2**, the solid-state magnetic susceptibility was measured on a polycrystalline sample at 2000 Oe over the temperature range of 2～300 K. A plot of the $\chi_M T$ *vs.* T susceptibility data for **2** is shown in Fig. 6. The value of $\chi_M T$ at 300 K is 8.80 emu mol$^{-1}$ K, which is slightly higher than the expected spin-only value for two Mn(II) ions (8.75 emu mol$^{-1}$ K). As the temperature is lowered, the $\chi_M T$ value decreases slowly to 8.75 emu mol$^{-1}$ K at 2 K. This indicates the presence of weak antiferromagnetic interactions within the sample.

The crystal packing of **2**, which is driven by hydrogen-bonding, reveals intermolecular Mn···Mn separation distance of 4.800 Å, regarding the intrachain Mn···Mn separation distance of 10.160 Å. And the Mn–Mn dinuclear fragment formed by the two Mn–COO···HO(H)–Mn paths is characterized by the shortest metal-metal separation distance (4.800 Å). Moreover, the magnetic exchange between transition metal centers through hydrogen-bonding interactions involving coordinated water molecules is well-exemplified in the literature[19, 20]. The Heisenberg spin Hamiltonian model ($\hat{H} = -JS_1S_2$, $S_1 = S_2 = 5/2$)[21, 22] for the isotropic magnetic exchange interaction in the dinuclear Mn(2) unit is given in Eq. (1).

$$\chi_M = \frac{2}{KT}\frac{Ng^2\beta^2}{B}\frac{A}{}$$

A = 55exp[30J/KT] + 30exp[20J/KT] + 14exp[12J/KT] + 5exp[6J/KT] + exp[2J/KT]

$$B = 1 + 11\exp[30J/KT] + 9\exp[20J/KT] + 7\exp[12J/KT] + 5\exp[6J/KT] + 3\exp[2J/KT] \quad (1)$$

A good fit was achieved with the fitting parameters as follows: $J$ = –0.23 $cm^{-1}$, $g$ = 2.004 and the agreement factor R = $\sum[(\chi_M)_{obs} - (\chi_M)_{calc}]^2/\sum(\chi_M)^2_{obs}$ is 1.08 × $10^{-5}$. The analysis confirms weak antiferromagnetic interactions between the Mn(II) atoms bridged by hydrogen-bonding. The hydrogen interactions provide an effective pathway for the magnetic exchange interaction between Mn(II) atoms. The small $J$ value observed may be explained by the fact that the magnetic orbitals are unfavorably oriented to interact.

### 3. 4 Thermogravimetric analyses of compounds 1 and 2

In order to further characterize compounds **1** and **2**, their thermal analyses were performed under $N_2$ atmosphere at a heating rate of 10 °C/min in the temperature range of 30～800 °C. As shown in Fig. 7, the TGA curves of **1** and **2** indicated that the samples undergo two main weight loss steps and the coordinated water molecules were lost in the ranges of 140～190 and 160～240 °C for **1** and **2**, respectively. The weight loss of 2.92% and 4.18% is consistent with the calculated values (2.81% and 4.01%). Then the framework began to decompose with continuous weight loss above 260 and 340 °C for **1** and **2**, respectively. The final residues of 29.63% (calcd. 30.06%) for **1** and 15.58% (calcd. 15.78%) for **2** may be the CdO and MnO powder, respectively. The results suggest that the backbone of **2** is more thermally robust than **1**, and can resist decomposition at temperature up to 340 °C.

### 3. 5 XRD analyses

In order to check whether the crystal structures are truly representative of the bulk materials, powder X-ray diffraction (PXRD) experiments were carried out for **1** and **2** at room temperature. As shown in Fig. 8, the peak positions of the simulated and experimental PXRD patterns are in agreement with each other, demonstrating that the bulk synthesized materials and the measured single crystals are the same.

## REFERENCES

(1) Luo, X. L.; Kan, L.; Li, X.; Sun, L. B.; Li, G. H.; Zhao, J.; Li, D. S.; Huo, Q. S.; Liu, Y. L. Two functional porous metal-organic frameworks constructed from expanded tetracarboxylates for gas adsorption and organosulfurs removal. *Cryst. Growth Des.* **2016**, 16, 7301–7307.

(2) Zheng, Y. Z.; Zheng, Z. P.; Chen, X. M. Two functional porous metal-organic frameworks constructed from expanded tetracarboxylates for gas adsorption and organosulfurs removal. *Coord. Chem. Rev.* **2014**, 258–259, 1–15.

(3) Sahoo, D.; Suriyanarayanan, R.; Chandrasekhar, V. A 30-membered nanonuclear cobalt(II) macrocycle containing phosphonate-bridged trinuclear subunits. *Cryst. Growth Des.* **2014**, 14, 2725–2728.

(4) He, H. M.; Sun, F. X.; Su, H. M.; Jia, J. T.; Li, Q.; Zhu, G. S. Syntheses, structures and luminescence properties of three metal-organic frameworks based on 5-(4-(2H-tetrazol-5-yl)phenoxy)isophthalic acid. *CrystEngComm.* **2014**, 16, 339–343.

(5) Zhang, K.; Qiao, Z. W.; Jiang, J. W. Molecular design of zirconium tetrazolate metal-organic frameworks for $CO_2$ capture. *Cryst. Growth Des.* **2017**, 17, 543–549.

(6) Wang, Z. J.; Qin, L.; Chen, J. X.; Zheng, H. G. H-Bonding interactions induced two isostructural Cd(II) metal-organic frameworks showing different selective detection of nitroaromatic explosives. *Inorg. Chem.* **2016**, 16, 10999–11005.

(7) Zhao, X. H.; Huang, X. C.; Zhang, S. L.; Shao, D.; Wei, H. Y.; Wang, X. Y. Cation-dependent magnetic ordering and room-temperature bistability in azido-bridged perovskite-type compounds. *J. Am. Chem. Soc.* **2013**, 135, 16006−16009.

(8) Wang, Y. F.; Li, S. H.; Ma, L. F.; Geng, J. L.; Wang, L. Y. Syntheses, crystal structures, and magnetic studies of two cobalt(II) coordination polymers based on concurrent ligand extension. *Inorg. Chem. Commun*. **2015**, 62, 42–46.

(9) Xu, W.; Si, Z. X.; Xie, M.; Zhou, L. X.; Zheng, Y. Q. Experimental and theoretical approaches to three uranyl coordination polymers constructed by phthalic acid and N,N´-donor bridging ligands: crystal structures luminescence, and photocatalytic degradation of tetracycline hydrochloride. *Cryst. Growth Des*. **2017**, 17, 2147–2157.

(10) Xu, C. X.; Zhang, J. G.; Yin, X.; Cheng, Z. X. Structural diversity and properties of M(II) coordination compounds constructed by 3-hydrazino-4-amino-1,2,4-triazole dihydrochloride as starting material. *Inorg. Chem.* **2016**, 55, 322–329.

(11) Wang, Y. F.; Li, Z.; Sun, Y. C.; Zhao, J. S.; Wang, L. Y. Structural modulation and properties of four cadmium(II) coordination architectures based on 3-(pyridin-4-yl)-5-(pyrazin-2-yl)-1H-1,2,4-triazol polycarboxylate ligands. *CrystEngComm*. **2013**, 15, 9980–9987.

(12) Sheldrick, G. M. *SHELXS-97, Program for X-ray Crystal Structure Determination*. University of Gottingen, *Germany* **1997**.

(13) Sheldrick, G. M. *SHELXL-97, Program for the Refinement of Crystal Structure*. University of Göttingen, *Germany* **1997**.

(14) Wang Y. F.; Sun, X. Y.; Geng, J. L. Synthesis, crystal structure and fluorescent properties of a cadmium(II) complex with 3-(pyridin-4-yl)-5(pyrazin-2-yl)-1H-1,2,4-triazole. *Chin. J. Struct. Chem.* **2016**, 35, 397–403.

(15) Chang, X. H.; Qin, J. H.; Ma, L. F.; Wang, J. G.; Wang, L. Y. Two-and three-dimensional divalent metal coordination polymer constructed from a new fricarboxylate linker and dipyridyl ligands. *Cryst. Growth Des.* **2012**, 12, 4649–4657.

(16) Tao, J.; Tong, M. L.; Shi, J. X.; Chen, X. M. Blue photoluminescent zinc coordination polymers with supertetranuclear cores. *Chem. Commun.* **2000**, 20, 2043–2044.

(17) Pérez-Bolívar, C.; Takizawa, S. Y.; Nishimura, G.; Montes, V. A.; Anzenbacher, P. High-efficiency tri(8-hydroxyquinoline)aluminum ($Alq_3$) complexes for organic white-light-emitting diodes and solid-state lighting. *Chem. Eur. J.* **2011**, 17, 9076–9082.

(18) Li, X.; Yang, L.; Zhao, L.; Wang, X. L.; Shao, K. Z.; Su, Z. M. Luminescent metal-organic frameworks with anthracene chromophores: small-molecule sensing and highly selective sensing for nitro explosives. *Cryst. Growth Des.* **2016**, 16, 4374–4382.

(19) Kozlevčar, B.; Kitanovski, N.; Jagličić, Z.; Bandeira, N. A. G.; Robert, V.; Guennic, B. L. Gamez, P. *Cis-trans* isomeric and polymorphic effects on the magnetic properties of water-bridged copper coordination chains. *Inorg. Chem*. **2012**, 51, 3094−3102.

(20) Tang, J. K.; Costa, J. S.; Golobic, A.; Kozlevcar, B.; Robertazzi, A.; Vargiu, A. V.; Gamez, P.; Reedijk, J. Magnetic coupling between copper(II) ions mediate by hydrogen-bonded (neutral) water molecules. *Inorg. Chem.* **200**9, 48, 5473–5479

(21) Fuller, A. L.; Watkins, R. W.; Dunbar, K. R.; Prosvirin, A. V.; Arif, A. M.; Berreau, L. M. Manganese(II) chemistry of a new N3O-donor chelate ligand: synthesis, X-ray structures, and magnetic properties of solvent- and oxalate-bound complexes. *Dalton Trans.* **2005**, 1891–1896.

(22) Kahn, O. *Molecular Magnetism*, VCH Publishers, *New York* **1993**.

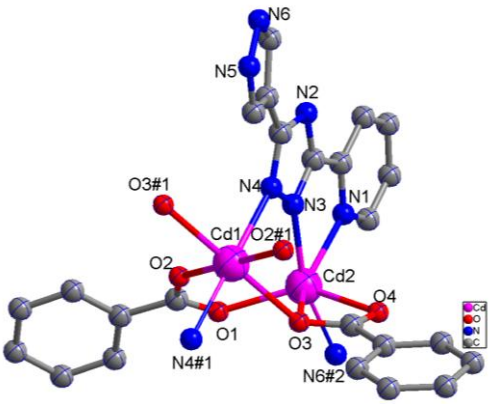


**Fig, 1. Coordination environment of Cd(II) ions in 1**

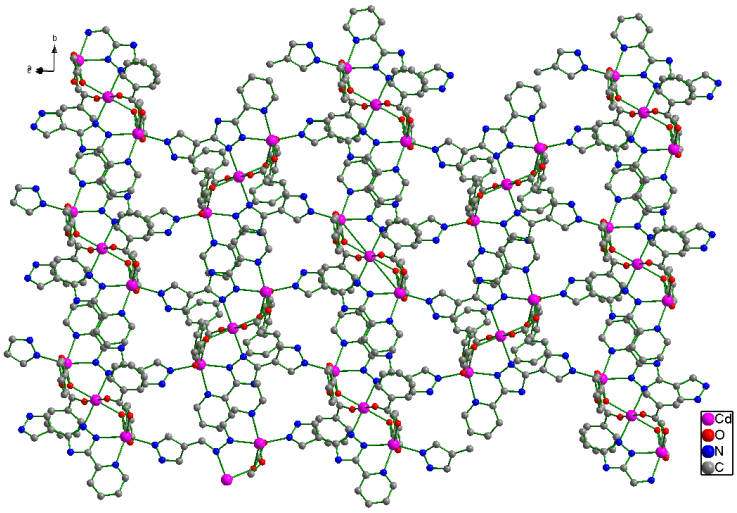


**Fig. 2. 2D network structure of 1**

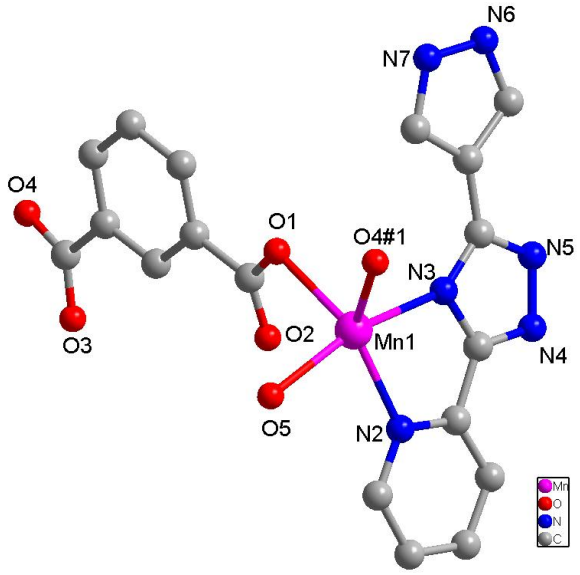


**Fig. 3. Coordination environment of the Mn(II) ion in 2**

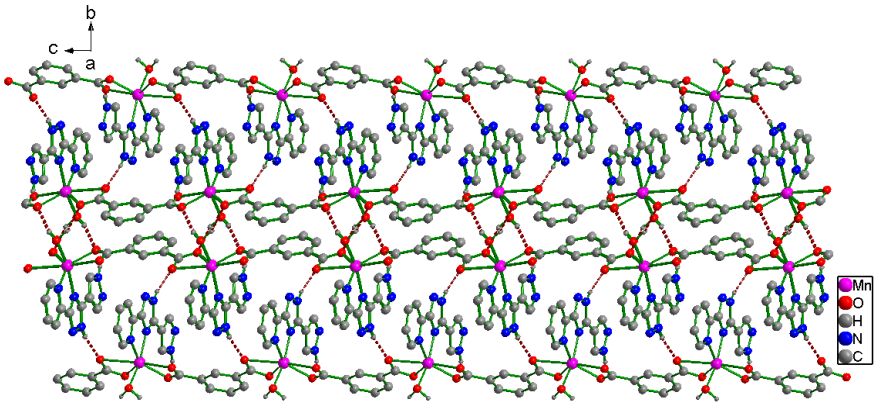


**Fig. 4. 3D supramolecule structure of 2**

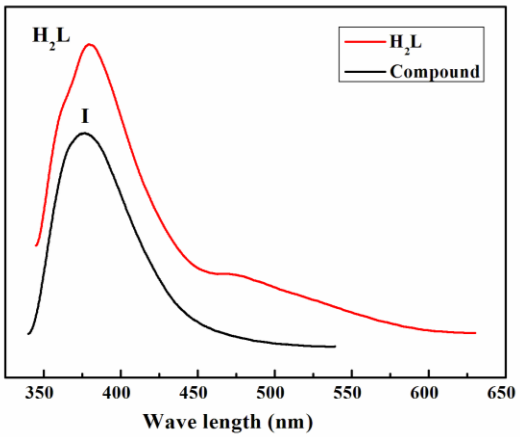


**Fig. 5. Emission spectra for 1 in the solid state**

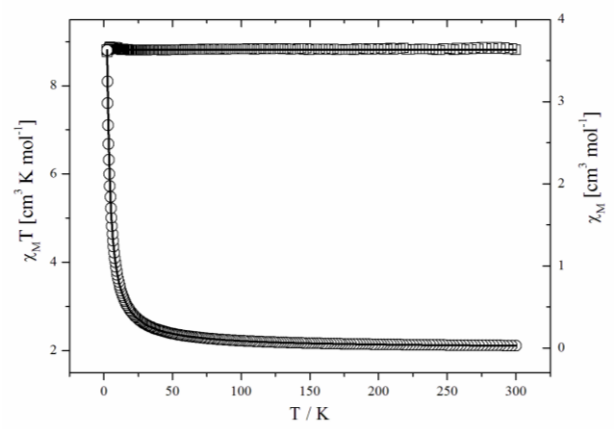


**Fig. 6. Temperature dependence of $\chi_M T$ (□) and $\chi_M$ (O) for 2 and their corresponding theoretical curves (solid lines)**

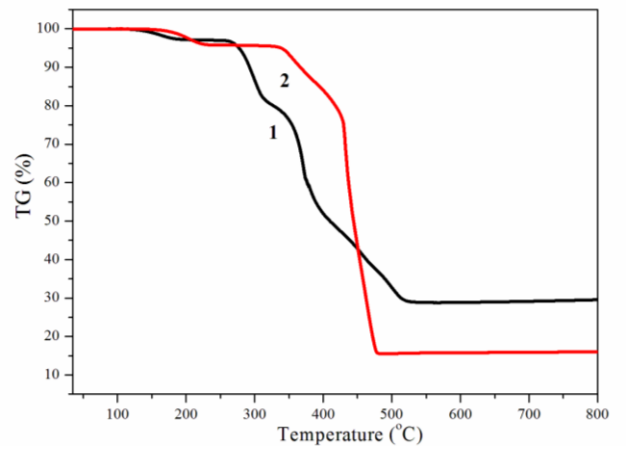


**Fig. 7. TGA curves of compounds 1 and 2**

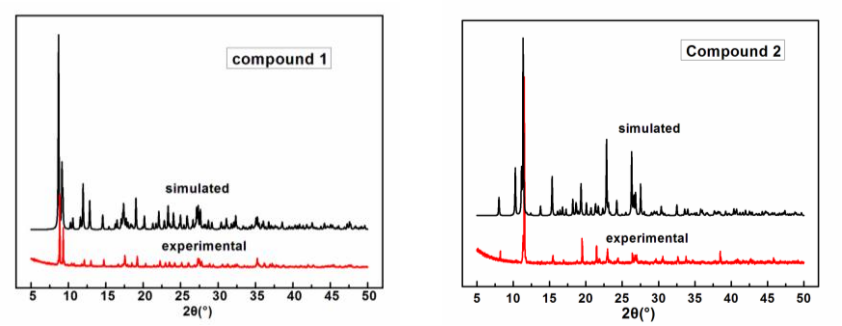


**Fig. 8. PXRD patterns of compounds 1 and 2**

**Table 1. Crystal Data and Details of Experiment for Compounds 1 and 2**

| Compounds | **1** | **2** |
|---|---|---|
| Empirical formula | $C_{24}H_{19}Cd_{1.5}N_6O_5$ | $C_{18}H_{14}MnN_6O_5$ |
| Formula weight | 640.05 | 449.29 |
| Temperature (K) | 293(2) | 293(2) |
| Crystal system | Monoclinic | Monoclinic |
| Space group | $P2_1/n$ | $P2_1/n$ |
| Cell parameters (Å, °) | a = 12.1665(3), $\alpha$ = 90<br>b = 11.4872(2), $\beta$ = 93.157(2)<br>c = 17.2589(4), $\gamma$ = 90 | a = 9.0415(5), $\alpha$ = 90<br>b = 22.0030(11), $\beta$ = 112.969(7)<br>c = 10.1605(7), $\gamma$ = 90 |
| Volume (Å$^3$) | 2408.43(9) | 1861.1(2) |
| $Z$ | 4 | 4 |
| Calculated density (g/cm$^3$) | 1.765 | 1.604 |
| Absorption coefficient (mm$^{-1}$) | 1.385 | 0.756 |
| $F$(000) | 1268.0 | 916.0 |
| Crystal size (mm$^3$) | 0.20 × 0.20 × 0.18 | 0.18 × 0.18 × 0.20 |
| 2$\theta$ range for data collection (°) | 6.666～51 | 7.06～51.998 |
| Index ranges | –14≤$h$≤14<br>–13≤$k$≤13<br>–20≤$l$≤20 | –11≤$h$≤12<br>–27≤$k$≤27<br>–13≤$l$≤12 |
| Reflections collected | 13177 | 11233 |
| Independent reflections | 4425 ($R_{int}$ = 0.0296) | 3648 ($R_{int}$ = 0.0475) |
| Data/restraints/parameters | 4425/0/334 | 3648/0/272 |
| Goodness-of-fit on $F^2$ | 1.034 | 1.057 |
| Final $R$ indexes ($I > 2\sigma(I)$) | $R$ = 0.0277, $wR$ = 0.0548 | $R$ = 0.0445, $wR$ = 0.0969 |
| Final $R$ indexes (all data) | $R$ = 0.0337, $wR$ = 0.0577 | $R$ = 0.0602, $wR$ = 0.1027 |
| Largest diff. peak and hole (e·Å$^{-3}$) | 0.35 and –0.37 | 0.35/–0.35 |

**Table 2. Selected Bond Lengths (Å) and Bond Angles (°) of Compounds 1 and 2**

| 1 | | | |
|---|---|---|---|
| Bond | Dist. | Bond | Dist. |
| Cd(1)–O(2)#1 | 2.332(2) | Cd(2)–O(1) | 2.1892(2) |
| Cd(1)–O(2) | 2.332(2) | Cd(2)–O(3) | 2.5890(2) |
| Cd(1)–O(3) | 2.3311(2) | Cd(2)–O(4) | 2.3173(2) |
| Cd(1)–O(3)#1 | 2.3311(2) | Cd(2)–N(1) | 2.403(2) |
| Cd(1)–N(4) | 2.317(2) | Cd(2)–N(3) | 2.261(2) |
| Cd(1)–N(4)#1 | 2.317(2) | Cd(2)–N(6)$^2$ | 2.315(2) |
| Angle | (°) | Angle | (°) |
| O(2)–Cd(1)–O(2)#1 | 180.0 | N(3)–Cd(2)–N(1) | 71.37(7) |
| O(3)–Cd(1)–O(2)#1 | 91.76(7) | N(3)–Cd(2)–N(6)#2 | 162.10(8) |
| O(3)–Cd(1)–O(2) | 88.24(7) | N(6)#2–Cd(2)–O(3) | 111.72(7) |
| **2** | | | |
| Bond | Dist. | Bond | Dist. |
| Mn(1)–O(1) | 2.1653(2) | Mn(1)–N(2) | 2.223(2) |
| Mn(1)–O(4)#1 | 2.1804(2) | Mn(1)–N(3) | 2.260(2) |
| Mn(1)–O(5) | 2.2175(2) | | |
| Angle | (°) | Angle | (°) |
| O(4)1–Mn(1)–O(5) | 95.96(7) | N(2)–Mn(1)–O(1) | 135.52(7) |
| O(1)–Mn(1)–O(5) | 92.42(7) | N(2)–Mn(1)–N(3) | 75.62(7) |
| O(1)–Mn(1)–O(4)#1 | 87.72(7) | N(3)–Mn(1)–O(1) | 95.80(7) |
| N(3)–Mn(1)–O(5) | 164.70(7) | N(2)–Mn(1)–O(5) | 89.48(7) |
| N(3)–Mn(1)–O(4)#1 | 97.24(7) | N(2)–Mn(1)–O(4)#1 | 136.25(7) |

Symmetry transformations used to generate the equivalent atoms: #1: 1–*x*, 1–*y*, 1–*z*; #2: –1/2+*x*, 1/2–*y*, –1/2+*z* for **1**; #1: *x y*, –1+*z* for **2**

# Syntheses, Crystal Structures and Characterization of Two Coordination Polymers Based on Mixed Ligands

WANG Yu-Fang(王玉芳)　HE Chao-Jun(何朝军)

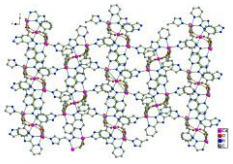

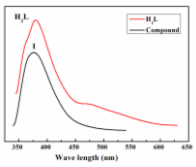

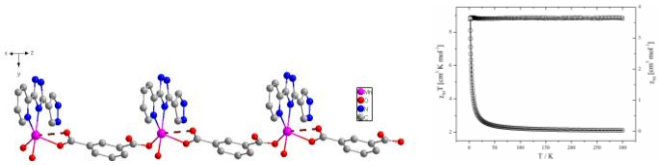

Compound **1** displays a two-dimensional plane structure consisting of $[Cd_3(bc)_2(HL)]$ subunits. Compound **2** possesses a one-dimensional chain structure and is further extended into a 3-D supramolecular architecture via hydrogen bonds. Photoluminescence studies showed compound **1** exhibits luminescent emissions with emission maxima at 375 nm. In compound **2**, the weak antiferromagnetic interactions between the Mn(II) atoms are bridged by hydrogen-bonding. The hydrogen interactions provide an effective pathway for the magnetic exchange interaction between Mn(II) atoms.